

PAPER

Empirical study of gradient lengths ratio η_e in the near SOL region in ASDEX Upgrade tokamak

To cite this article: H J Sun *et al* 2020 *Plasma Phys. Control. Fusion* **62** 025005

View the [article online](#) for updates and enhancements.



IOP | ebooks™

Bringing you innovative digital publishing with leading voices to create your essential collection of books in STEM research.

Start exploring the collection - download the first chapter of every title for free.

Empirical study of gradient lengths ratio η_e in the near SOL region in ASDEX Upgrade tokamak

H J Sun^{1,2} , E Wolfrum², T Eich² , A Kallenbach² , P Schneider²,
B Kurzan², U Stroth^{2,3} and the ASDEX Upgrade Team

¹ United Kingdom Atomic Energy Authority, Culham Centre for Fusion Energy, Culham Science Centre, Abingdon, Oxon, OX14 3DB, United Kingdom

² Max Planck Institute for Plasma Physics, Garching, Germany

³ Physik-Department E28, Technische Universität München, Garching, Germany

E-mail: hongjuan.sun@ukaea.uk

Received 8 August 2019, revised 3 October 2019

Accepted for publication 29 October 2019

Published 20 November 2019



CrossMark

Abstract

A survey of the correlation between density and temperature gradient lengths (λ_{ne} and λ_{Te}) has been performed for the near SOL regions in the ASDEX Upgrade tokamak. In common with previous studies, the ratio of the near SOL density and temperature gradient lengths, $\eta_e = \lambda_{ne}/\lambda_{Te}$, is found to be close to unity across a wide range of plasmas. However, it is found that it is possible for both the density and temperature gradients to vary separately without varying the other greatly. The empirical results show that the correlation between density and temperature profiles in the near SOL is related to the divertor regimes. In the linear/sheath limited regime, the density and temperature profiles are closely correlated, η_e is observed to be close but slightly less than unity. In the high recycling/conduction limited regimes, which is the most common case for ASDEX Upgrade plasma, λ_{ne} and λ_{Te} are correlated due to a common dependence on q_{95} or, equally, I_p . A weak dependence of η_e on separatrix temperature is observed in this regime. Since the separatrix temperature depends only weakly on the power density flowing through the SOL and the variation is very small, a small variation of η_e is observed. For ASDEX Upgrade, it lies between 1 and 2 for most of discharges in the conduction limited regime. In the detached regime very high η_e , of up to 6, are observed. This is associated with the transition to the high density limit where convective transport due to filaments dominates particle transport resulting in very flat density profiles. At the same time, temperature profiles are observed to be unchanged.

Keywords: tokamak, SOL, gradient length ratio

(Some figures may appear in colour only in the online journal)

1. Introduction

The electron density and temperature decay lengths in the scrape-off layer (SOL), λ_{ne} and λ_{Te} , set crucial boundary conditions for the heat- and particle-handling in magnetically confined plasmas. These decay lengths control the penetration of recycling hydrogen neutrals and edge-produced impurities into the plasma. How edge temperature and density profiles correlate eventually determines the characteristics of edge pressure. The density and temperature gradient length ratio,

$\eta_e = \lambda_{ne}/\lambda_{Te}$, is also important in transport physics and determining turbulence characteristics.

A previous study on ASDEX Upgrade (AUG), found a fairly constant η_e close to 2 from pedestal across to the SOL for a series of Type I ELMy H-mode discharges [1]. For a larger data set of AUG ELMy H-modes, η_e in the pedestal region was observed to be $\eta_e = 1.9 \pm 0.6$ [2]. These studies [1, 2] were carried out with graphite plasma facing components (PFCs). A more recent study, for a database of AUG Type I ELMy H-mode plasma with tungsten PFCs, found η_e

to range from $\eta_e = 1 - 2$ in both the pedestal and SOL regions, with an average value of $\eta_e \approx 1.4$ [3]. A study of η_e in the SOL for a data set of JET ELMy H-mode plasma found an average value of $\eta_e \approx 1.5$ [4]. The study of a large data set of DIII-D plasmas, including different high confinement plasma scenarios, found that η_e in the middle of the pedestal ranged from $\eta_e = 1 - 3$ [5]. For a Tore Supra data set of Ohmic limiter discharges [6], the temperature gradient length in the SOL region is found to be generally larger than the density gradient length, with a rough relation of $\lambda_{T_e} \approx 1.4(\pm 1)\lambda_{n_e}$, giving $\eta_e \approx 0.7$.

Combining previous studies, η_e is observed to be not far from unity in the edge plasma, suggesting that the density and temperature profiles may be closely coupled. However, η_e varies in the range $\eta_e \approx 0.4 - 3$, across the single machine datasets and between different machines. The confidence intervals for the measurements of SOL gradients for some of the studies are relatively large, resulting in confidence intervals in η_e comparable to the observed scatter. Hence, it is useful and important to document the empirical parametric dependences of η_e and find out whether the temperature and density profiles are always coupled.

Recent improvements of the AUG Thomson scattering (TS) system [7] enable the detailed study of characteristics in the near SOL profiles. The purpose of this paper is to study the relation between edge T_e and n_e profiles in the SOL regions. The rest of this paper is organized as follows: The experimental methods and datasets are briefly introduced in section 2. In section 3, at first, the dependences on plasma global parameters are tested; then, the correlations with local parameters are checked; at last, the examples where the temperature and density profiles are decoupled are presented. In section 4, the results are summarized and physics implications are discussed.

2. Experimental methods and database

In ASDEX Upgrade, electron temperature and density profiles can be obtained simultaneously for one discharge by a vertical TS system [3, 7]. The system is equipped with 4 Nd:YAG lasers at 1064 nm for core profiles and 6 lasers for the edge plasma. The system has a spatial resolution of 25 mm and temporal resolution of 80 Hz in the core and a spatial resolution of around 3 mm and temporal resolution of 120 Hz in the near SOL.

Since the 2014 AUG campaign, significant improvements of the TS system have enabled good measurements of the SOL temperature and density profiles [3]. The Type I ELMy H-mode discharges under attached divertor condition (36 in total) and L-mode attached discharges (27 in total) used in the present dataset are the same discharges as those used in [8]. In H-mode plasma, during ELMs the thermocurrents measured in the divertor are strongly increased, which indicates the onset of an ELM. The SOL profiles immediately prior to the ELM onset is taken by averaging data over time windows from 3.5 to 1.5 ms prior to each ELM onset, but at least 4 ms following the onset of the previous ELM. Data

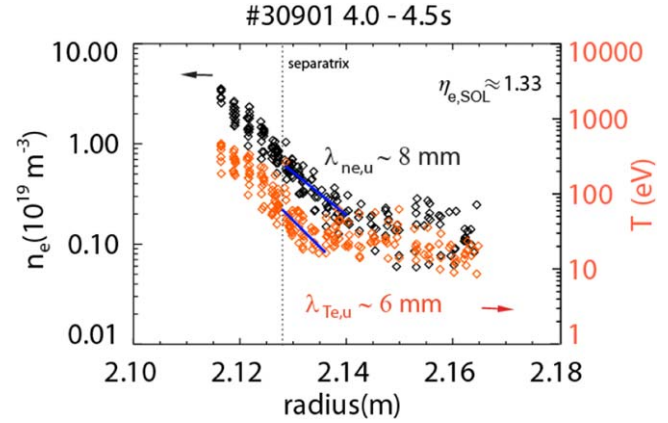


Figure 1. Log plot of electron temperature (in red) and density (in black) versus radius for AUG discharge #30901. The (solid blue) line fit to near SOL data gives the gradient decay lengths. The dashed line the separatrix indicates the separatrix position.

from the 1.5 ms period prior to each ELM onset are excluded, to ensure no data is included from the ELM event itself due to possible errors in the ELM recognition and time delays between different diagnostics. Data from within 4 ms of the previous ELM onset are excluded, to ensure the profiles have sufficiently recovered from the previous ELM. The same method is not applicable for the inter-ELM profiles under the detached condition because the ELM frequency is too high. For detached plasmas, profiles are collected across the whole time window as the perturbation to the profiles from each ELM crash are relatively small.

Figure 1 gives typical profiles for an AUG discharge. Both temperature (in red) and density (in black) profiles normally exhibit a two-layer structure. Close to the separatrix, in the so-called near SOL, it has a steep exponential decay. Beyond this region, in the so-called far SOL, the profile has an exponential decay with much longer scale length. The temperature and density decay length $\lambda_{T_{e,u}}$ and $\lambda_{n_{e,u}}$ in this paper refer to the first e-folding length in the profiles, that is why they are also called midplane e-folding distance in some studies. The solid blue line fit to the log plot of near SOL data gives the gradient decay lengths in figure 1.

3. Experimental observations of the correlation between density and temperature profiles

3.1. General observation and dependences on global parameters

A previous study, with a database of Type I ELMy H-mode plasmas, found the near SOL density and temperature profiles are closely correlated with η_e in the range from $\eta_e = 1 - 2$, with an average value of $\eta_e \approx 1.4$ [3]. To increase the range of the plasma parameters for the parametric dependence study, L-mode discharges under attached divertor conditions are also included in this paper. Figure 2 shows a plot of $\lambda_{T_{e,u}}$ versus $\lambda_{n_{e,u}}$ in the near SOL for both H-mode and L-mode discharges in the present study. Most of the discharges have η_e have values in the range 1–2, as shown by the solid black

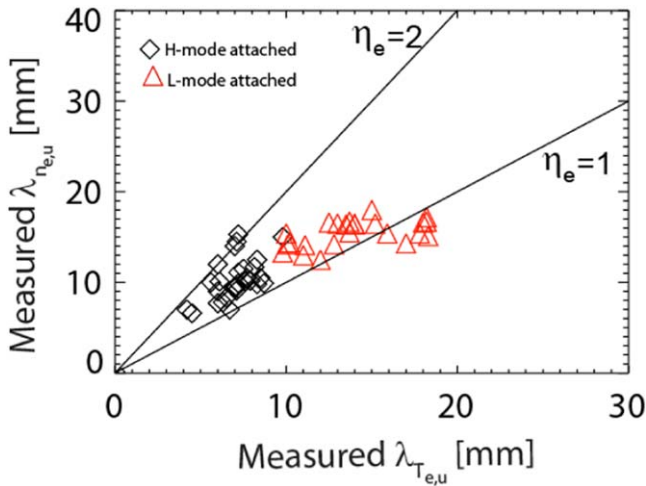


Figure 2. $\lambda_{n_{e,u}}$ versus $\lambda_{T_{e,u}}$ for both H-mode and L-mode discharges. Upper line corresponds to η_e of 2 and lower line to η_e of 1.

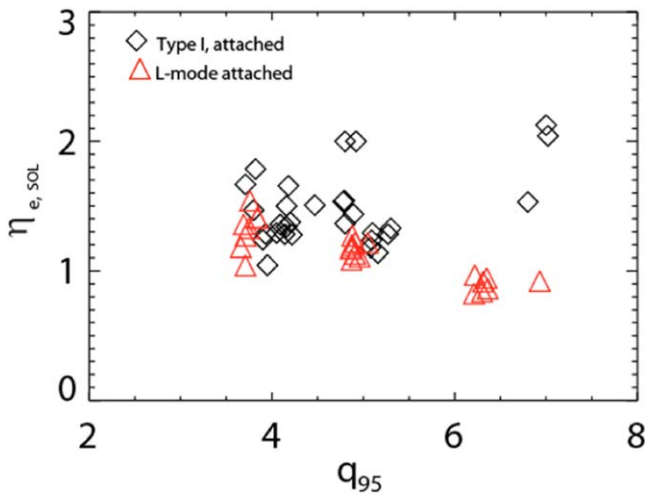


Figure 3. η_e against safety factor q_{95} in the near SOL region, for the AUG SOL dataset.

lines. However, there are data from L-mode discharges which lie below one, i.e. $\lambda_{T_{e,u}} > \lambda_{n_{e,u}}$. In the next section, it will be shown that these discharges are associated with very low separatrix density. The previous studies from both IR camera and TS system measurements show that the SOL characteristic temperature and power decay lengths have a strong plasma current, I_p , dependence [3, 8, 9]. Detailed analysis in both H- and L-mode plasma from TS measurements suggests that a safety factor, q_{95} , dependence may be more appropriate to describe the temperature gradient length scaling [3, 8]. Do these global plasma parameters still play an important role in determining the gradient length ratio? This AUG dataset contains only a limited range in B_T and the majority of the dataset for both L-mode and H-mode is comprised of discharges around 2.5 T. Thus, I_p and q_{95} are strongly correlated. Since q_{95} is directly related to important SOL parameters, such as connection length, only the correlation with q_{95} will be discussed in the following sections. Plots of η_e against q_{95} are shown in figure 3. For H-mode plasma, there is no correlation between η_e and q_{95} . For the L-mode plasma, for the

discharges with $q_{95} < 6$, there is no correlation between η_e and q_{95} . However, η_e for the discharges with $q_{95} > 6$ ($I_p \approx 600$ kA) clearly drops below unity, giving a negative trend between η_e and q_{95} . These discharges with higher q_{95} are the same ones mentioned above which will be discussed more in the next section.

As observed in the previous study of SOL temperature profile [8], $\lambda_{T_{e,u}}$ has a strong q_{95} dependence, $\lambda_{T_{e,u}} \propto q_{95}$ for both H-mode and L-mode plasmas. As can be seen from figures 4(a) and (b), $\lambda_{n_{e,u}}$ also has a strong q_{95} dependence, $\lambda_{n_{e,u}} \propto q_{95}$, for H-mode plasma. For L-mode plasma with $q_{95} < 6$, there is a similar positive trend between $\lambda_{n_{e,u}}$ and q_{95} . For $q_{95} > 6$, there is little evidence for a dependence of $\lambda_{n_{e,u}}$ on q_{95} and certainly not one that lies outside the measurement errors. Overall, the correlations between $\lambda_{n_{e,u}}$ and q_{95} are consistent with the observed relation between η_e and q_{95} . In particular, the lack of a dependence of η_e on q_{95} , for H-mode plasma and L-mode plasma with $q_{95} < 6$, results from a co-dependence of $\lambda_{n_{e,u}}$ and $\lambda_{T_{e,u}}$ on q_{95} .

3.2. Dependences on local parameters

In this section, the correlation between η_e and the separatrix local parameters will be examined. In figure 5(a), for H-mode attached plasmas, η_e is seen not to correlate with $n_{e,sep}$. For example, η_e with $n_{e,sep} \approx 1.5 \times 10^{19} \text{ m}^{-3}$ lies in almost the same range as that with $n_{e,sep} \approx 5.5 \times 10^{19} \text{ m}^{-3}$. For L-mode plasma, the discharges with smallest $\eta_e \leq 1$ are those with lowest density. As discussed in the previous section, these discharges with the lowest density do not follow the generally observed positive trend between $\lambda_{n_{e,u}}$ and q_{95} . The target temperature for these discharges is very high, $T_t \geq 30$ eV and comparable with upstream temperature T_u . The weak temperature difference between the upstream and target implies that the divertor is in the linear/sheath limited regime [10, 11]. In a previous study [12], η_e in the pedestal region is observed to lie mainly between 1 and 3 across the entire data set from AUG, JET and DIII-D, as shown in figure 7.43 in [12]. However, there are several discharges that fall outside of this range, with very low pedestal density, $n_{e,ped} \approx 1 - 1.5 \times 10^{19} \text{ m}^{-3}$, the gradient length ratio is also close but slightly less than unit, $\eta_e \leq 1$. These discharges are also found to be in the linear/sheath limited regime. A positive trend of higher separatrix temperature, $T_{e,sep}$, being associated with a larger η_e in the near SOL region is seen, figure 5(b), similar to the observation for the pedestal region [12]. In Tore Supra [6], a rough relation, $\lambda_{T_e} \approx 1.4 \lambda_{n_e}$, is found between the density and temperature decay length in the SOL, equivalent to $\eta_e \approx 0.7$. Across this Tore Supra database, the separatrix temperature is about 30 eV. Thus, the lower η_e in the Tore Supra study appears consistent with the trend observed in figure 5(b). The dependence of η_e on $T_{e,sep}$ could be explained that, when cross-field transport remains the same, the reduction of parallel heat transport due to the lower temperature will broaden λ_{T_e} , thus leading to a smaller η_e . Unlike the result from pedestal region, there is no obvious correlation between η_e and the SOL collisionality, $\nu_{SOL,e}^* \approx 10^{-16} n_{e,u} L / T_{e,u}^2$ [13], over the analyzed dataset, figure 5(c). In the study of the pedestal region [12], a negative correlation between η_e and the

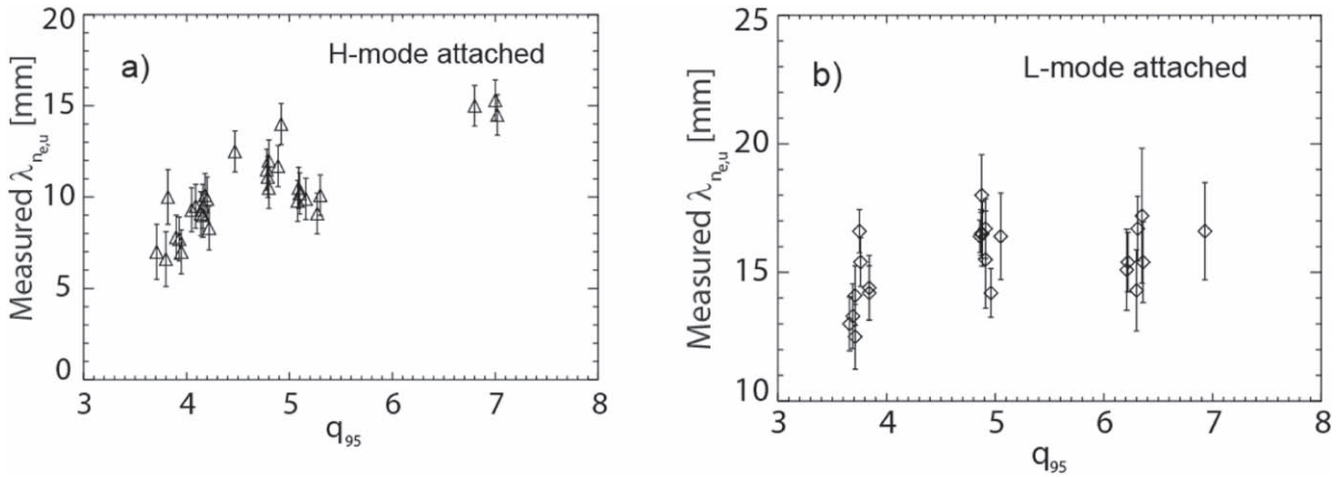


Figure 4. $\lambda_{n_{e,u}}$ versus q_{95} (a) for H-mode plasma; (b) for L-mode plasma.

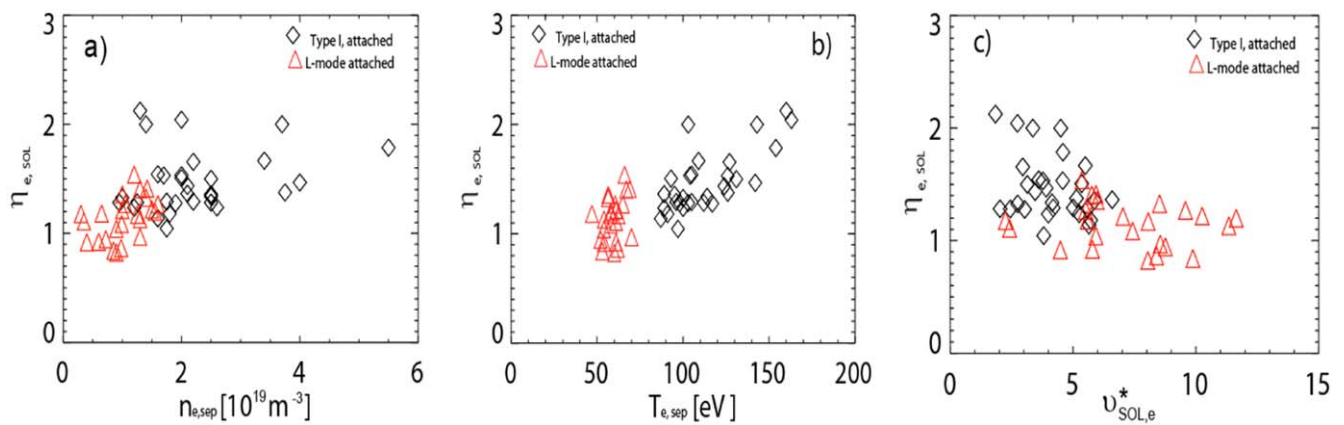


Figure 5. η_e in the near SOL plotted against (a) separatrix density, $n_{e, \text{sep}}$, (b) separatrix temperature, $T_{e, \text{sep}}$, (c) SOL collisionality, $u_{\text{SOL}, e}^*$, for the AUG SOL dataset.

collisionality, $v_{\text{ped}, e}^*$, was identified for all analyzed data. The fact that there is correlation observed between η_e and local collisionality in the pedestal region, but not in the SOL region, could be due to the change of the particle transport channel in the SOL region.

3.3. Studies where temperature and density gradient lengths change separately

The results from previous sections show that the measured η_e in the near SOL region is not far from unity for both H-mode and L-mode plasmas. Even when the plasma transits from the L-mode regime to the H-mode regime, the temperature and density profiles become steeper simultaneously and there is no sudden increase of η_e from L-mode to H-mode. This gives the impression that a coupling between the density and temperature profiles exists, in the sense that the gradient length of one cannot be changed alone. To study whether this is the case, this section presents a study of two plasma regimes which have been identified as having a relatively wider range in one of the gradient lengths whilst having a relatively small range in the other.

An alternative improved confinement regime to the H-mode is the so-called improved energy confinement regime (I-mode) [14–17]. In the formation of I-mode plasmas, an increase of the edge temperature with a concomitant steepening of the edge gradients builds a temperature pedestal similar to that of the H-mode. However, the edge density profile remains almost unchanged, with an edge density profile very similar to that of the L-mode. Thus, the transition to I-mode plasma provides a good way to investigate the correlation of the temperature profile with the gradient length ratio, for constant plasma density.

An example of an AUG I-mode discharge, #30865, is described in detail in [16]. In this discharge, the ECRH heating power was increased every 500 ms, while the density remained almost constant. Around $t \approx 3.18$ s, the electron temperature and pressure gradients slightly steepen and the confinement increases slightly at constant heating power. This spontaneous confinement transition is considered as a transition to a weak I-mode. With additional heating power, at $t = 3.5$ s, $H_{98(y,2)}$ increases above 0.6 and a clear I-mode develops: the electron temperature gradient strongly increase, while the density gradient remains almost unchanged. A more detailed analysis of the plasma behavior for each of these

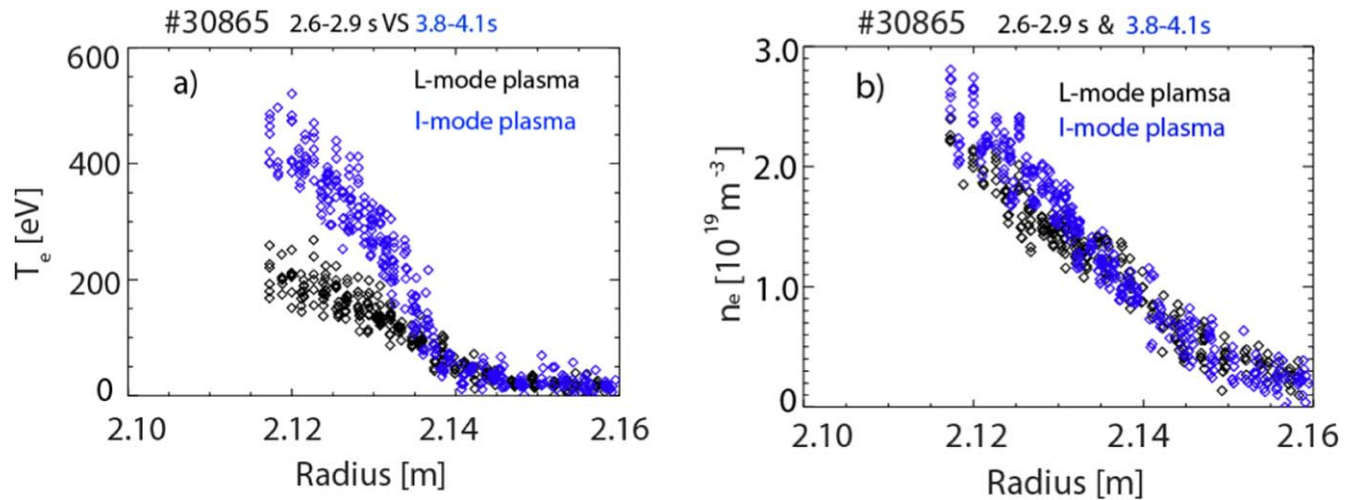


Figure 6. (a) Electron temperature T_e and (b) electron density against major radius at the midplane for the L-mode (black), and strong I-mode (blue) phases of AUG discharge #30865.

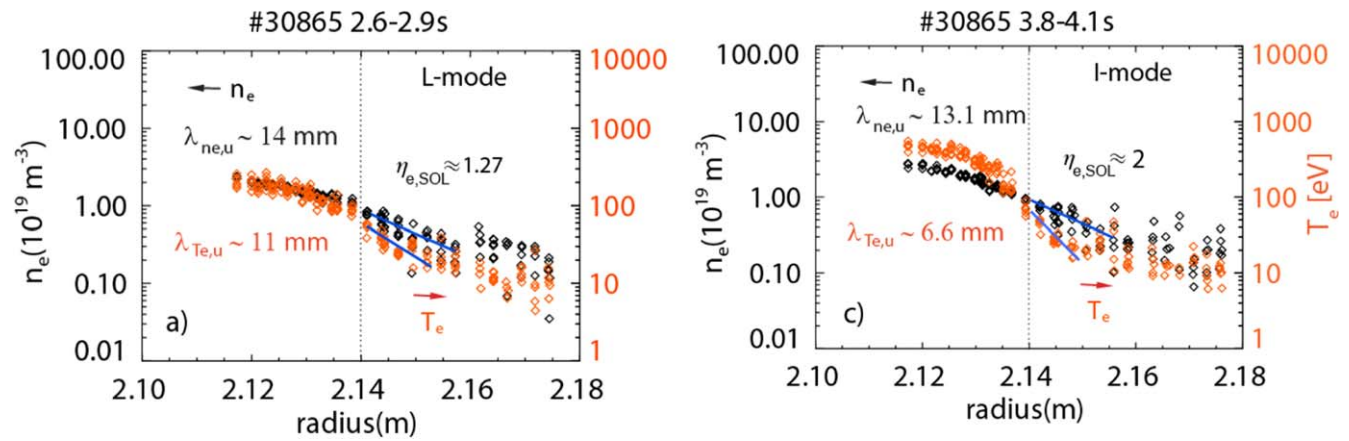


Figure 7. Log plot of electron temperature and density versus radius in the edge region for L-mode plasma (black), I-mode plasma (red) of the same AUG discharge as figure 6. The black dashed lines indicate the position of separatrix.

three phases is presented in [16]. Here, only the change of temperature and density profiles in L-mode and strong I-mode phases are discussed to demonstrate how η_e can change only due to a change of the temperature profile. The evolution of the temperature and density profiles from L-mode to strong I-mode is illustrated in figures 6 and 7. The L-mode phase has $\eta_e \approx 1.27$, in the I-mode regime, η_e increases, to $\eta_e \approx 2$. This I-mode discharge demonstrates how changes in the temperature profile affect the gradient length ratio. As the temperature profile becomes much steeper, while the density profile remains almost unchanged, the gradient length ratio η_e increases.

Assuming Spitzer–Harm transport along the field lines, the calculated separatrix temperature, $T_{e,sep}$ is about 50 eV for the L-mode phase and around 80 eV in the strong I-mode phase. Although similar positive trends between η_e and local electron temperatures are observed in the I-mode regime, given the same $T_{e,sep}$, η_e in the I-mode plasma is higher than that in typical L- and H-mode plasma. This could be due to the fact that in I-mode, a weakly coherent mode, which is located very close to the separatrix, increases dominantly particle transport [15–17].

The next case is that of the transition of a H-mode plasma from attachment to detachment and then its approach to the H-mode density limit. In this case, the temperature gradient length is relatively constant compared to the change in the density gradient length. Figure 8 shows the characteristic time traces of an H-mode density limit discharge. Around $t \approx 2$ s, the plasma transits from the L-mode regime to the H-mode regime, due to the increase of heating power. During the H-mode regime, due to fueling without the cryo-pump, both the divertor neutral density and the electron density increases dramatically. Around $t \approx 3$ s, the divertor is detached, and the density continues increasing until it reaches the H-mode density limit around $t \approx 4$ s, when it triggers the H–L back transition shortly before the plasma collapses. Temperature and density profiles from four different phases of this discharge are shown in figure 9.

In the L-mode regime (figure 9(a)), with $n_{e,sep} \approx 1.5 \times 10^{19} \text{ m}^{-3}$, the temperature and density profiles have very similar gradient lengths, giving $\eta_{e,SOL} \approx 1$. After transition into H-mode (figure 9(b)), both the temperature and density gradient lengths decrease. λ_{T_e} decreases more than λ_{n_e} and so η_e increases to $\eta_{e,SOL} \approx 1.33$. The separatrix density also

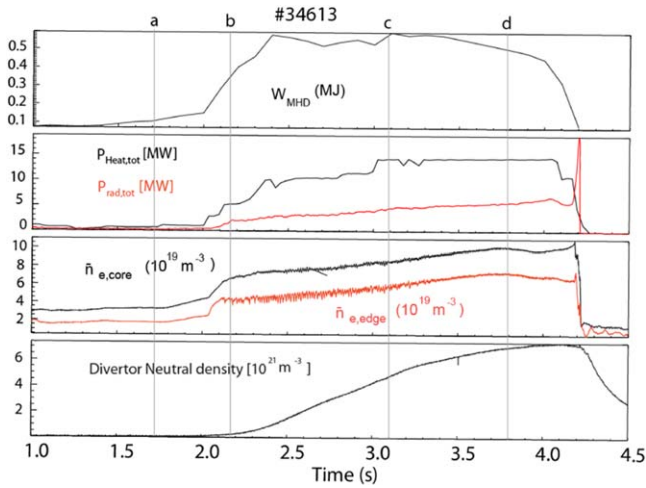


Figure 8. Time traces for AUG discharge #34613: plasma stored energy (W_{MHD}), total heating power and total radiation ($P_{Heat,tot}$ and $P_{rad,tot}$), line integrated edge and core electron density ($\bar{n}_{e,edge}$ and $\bar{n}_{e,core}$), divertor neutral density.

increases to $n_{e,sep} \approx 3.1 \times 10^{19} \text{ m}^{-3}$. At the time of the H-mode under detached divertor conditions (figure 9(c)), the divertor neutral pressure has continued to increase and the separatrix density has increased correspondingly [18] to $n_{e,sep} \approx 4.4 \times 10^{19} \text{ m}^{-3}$. The density profile has become much flatter and so η_e has increased further to $\eta_{e,ped} \approx 4.4$. Just before the H–L back transition (figure 9(d)), $n_{e,sep}$ has increased up to $n_{e,sep} \approx 6 \times 10^{19} \text{ m}^{-3}$. The pedestal top density has also increased, whilst the pedestal and SOL temperature have decreased. Due to the drop of $T_{e,sep}$, the temperature profile in the SOL also becomes slightly flatter, $\lambda_T \approx 11 \text{ mm}$. In this phase of the discharge, η_e is around 6. As can be seen from the evolution of profiles, the significant increase of η_e is caused primarily by the flattening of density profile. This feature of density profile flattening in the SOL region under detached divertor condition was observed in earlier studies of L-mode plasmas, where the phenomenon has been called the L-mode high density transition (HDT) [19]. The HDT occurs when the Greenwald density fraction, f_{GW} , is larger than a certain value. At this time, the density profile in the SOL changes: flattening its gradient and giving rise to a ‘shoulder’. In a recent study [20], it was shown that plasma filaments arise after the HDT as a result of the interchange instability. These filaments enhance perpendicular particle transport. It seems that these convective structures do not significantly enhance the heat transport, as shown in figure 9(c), suggesting that conductive transport remains the dominant cross-field heat transport mechanism. Only when the separatrix temperature decreases because of the increase of density does the slowing of parallel transport flatten the temperature profile in near SOL, figure 9(d).

4. Summary

A survey of the correlation between temperature and density gradient length for the near SOL region has been performed for

both H- and L-mode regimes in the ASDEX Upgrade tokamak. For both H- and L-mode plasmas, the majority of the gradient length ratio η_e lies between 1 and 2. However, there are data from L-mode discharges which lie below one. These low η_e L-mode discharges are found to be associated with very low density and relatively high target temperature, thus, are more likely in linear/sheath limited divertor regime. In a previous study, η_e in the pedestal region was observed to lie mainly between 1 and 3 across the entire data set from AUG, JET and DIII-D, as shown in figure 7.43 in [21]. However, there were also several discharges that fall outside of this range, with very low pedestal density, and the gradient length ratio for these is also $\eta_e \leq 1$. This suggests that, in the linear regime, the correlation between upstream temperature and density profiles also has influence into the pedestal region. Excluding those very low density L-mode discharges, the majority of data should be in the high recycling/conduction limited regime [3, 8]. In the conduction limited regime, there is no obvious correlation between η_e and global plasma parameters, q_{95} or I_p . This could be explained by both λ_{ne} and λ_{Te} having similar dependence on these global parameters. A weak positive trend of higher separatrix temperature $T_{e,sep}$ being associated with a larger η_e in the near SOL region is observed, this can be explained that by assuming that the cross-field transport depends only weakly on $T_{e,sep}$. In this case, increased $T_{e,sep}$ will result in reduced λ_{Te} and so increased η_e due to the positive temperature dependence of the Spitzer–Harm dominated parallel heat transport. In Tore Supra [6], a rough relation of $\lambda_{Te} \approx 1.4 \lambda_{ne}$ is found between the density and temperature decay lengths in the SOL, equivalent to $\eta_e \approx 0.7$. Across this Tore Supra database, the separatrix temperature is about 30 eV. Thus, the lower η_e in the Tore Supra study appears consistent with the trend observed in AUG. No obvious correlation with separatrix density and collisionality is observed.

For most data, η_e is not far from unity, suggesting that, changing the gradient length of one would affect the other and it is not likely to control these density and temperature profiles separately. However, regimes and conditions have been identified where the temperature and density profile length scales, and presumably the heat and particle transport, are not coupled. During the transition from the L-mode to the I-mode regime, a relatively large increase of η_e is associated with the temperature profile becoming much steeper while the density profile remains unchanged. During the I-mode phase, a dependence of η_e on temperature alone is also observed: larger η_e being associated with higher local temperature. However, with the same $T_{e,sep}$, $\eta_{e,SOL}$ in I-mode regimes are larger than those in similar H- and L-mode regimes. Under detached divertor conditions, the high density transition (HDT) occurs. Filaments appear, as a result of the interchange instability, which strongly enhance perpendicular particle transport, resulting in a very flat density profiles [20]. For the discharges studied here, these convective structures have small influence on heat transport and so the temperature gradient length remains almost constant. Thus, η_e can reach very high values, up to 6 for the H-mode case studied. Taken together, the I-mode transition and HDT demonstrate that the electron density and temperature gradients in the SOL can vary

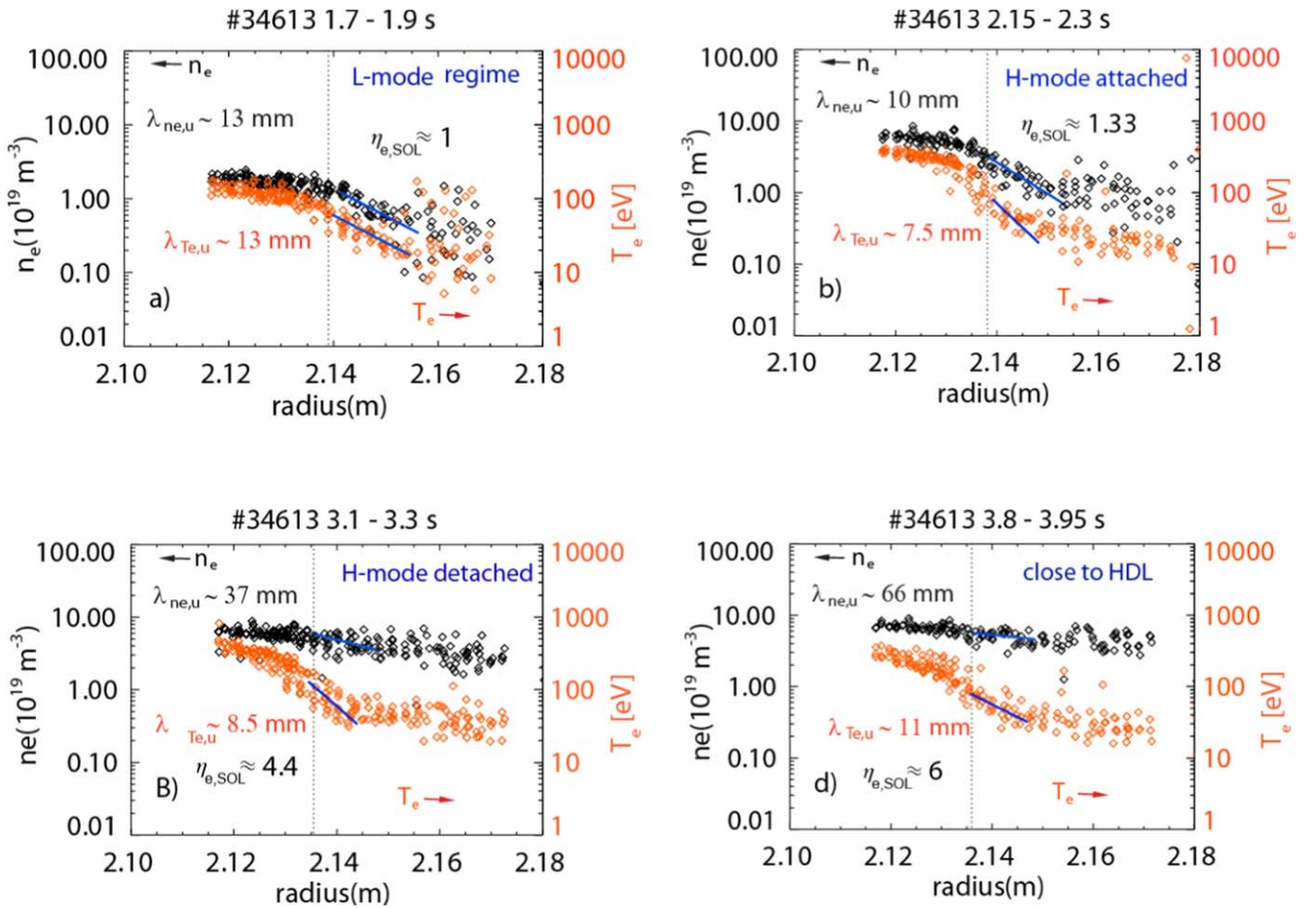


Figure 9. Log-linear plot of the electron temperature and density profiles, for the same AUG discharge as in figure 8, (a) in the L-mode regime; (b) at the beginning of H-mode regime, $n_{e,sep} \approx 3.1 \times 10^{19} \text{ m}^{-3}$; (c) in the middle of H-mode regime, $n_{e,sep} \approx 4.4 \times 10^{19} \text{ m}^{-3}$; and (d) at the end of H-mode, just before H-L back transition, $n_{e,sep} \approx 6.0 \times 10^{19} \text{ m}^{-3}$.

Table 1. Divertor, SOL and confinement regimes in this study of AUG plasma and the associated η_e .

Divertor/SOL regime	Confinement mode	SOL temperature and density profiles	η_e
Attached/Sheath limited	L-mode	Temperature and density closely coupled	$\eta_e \leq 1$
Attached/Conduction limited	L/H-mode	Both λ_{ne} and λ_{Te} depend on q_{95} or equivalently I_p .	$1 < \eta_e < 2$
	I-mode	Temperature pedestal similar to that of the H-mode, with an edge density profile very similar to that of the L-mode.	$\eta_e > 2$
Detached	L/H-mode	After shoulder formation in the near SOL density profile.	$\eta_e \gg 2$

independently. Thus, it has been demonstrated that the general correlation between them is due to co-dependence on other parameters and not due to a direct link. However, it remains the case that across the wide database of L-mode and H-mode discharges, sufficiently below the density limit, lie in the range $1 < \eta_e < 2$ in the ASDEX Upgrade tokamak. The divertor, SOL and confinement regimes in this study is summarized in table 1 along with the SOL temperature and density profile behavior and the associated η_e .

Far from being always strongly correlated, the SOL electron density and temperature gradient lengths have been shown to vary between and within SOL and global confinement regimes. This provides opportunities for optimizing the performance of




fusion power plants and a wealth of phenomena requiring theoretical explanation. Such an explanation requires a first principles understanding of the underlying mechanisms for particle and thermal transport in the SOL and their interplay with neutral particles. It is hoped that the results presented here will encourage further experimental and theoretical studies.

Acknowledgments

This work has been carried out within the framework of the EUROfusion Consortium and has received funding from the Euratom research and training programme 2014–2018 and

2019–2020 under grant agreement No 633053 and from the RCUK [grant number EP/T012250/1]. To obtain further information on the data and models underlying this paper please contact PublicationsManager@ukaea.uk*. The views and opinions expressed herein do not necessarily reflect those of the European Commission.

ORCID iDs

H J Sun  <https://orcid.org/0000-0003-0880-0013>
T Eich  <https://orcid.org/0000-0003-3065-8420>
A Kallenbach  <https://orcid.org/0000-0003-0538-2493>

References

- [1] Neuhauser J 2002 *Plasma Phys. Control. Fusion* **44** 855
- [2] Kallenbach A *et al* 2003 *Nucl. Fusion* **43** 573
- [3] Sun H J *et al* 2015 *Plasma Phys. Control. Fusion* **57** 075005
- [4] Eich T *et al* 2018 *Nucl. Fusion* **58** 034001
- [5] Groebner R *et al* 2006 *Plasma Phys. Control. Fusion* **48** A109
- [6] Fedorczak N *et al* 2017 *Nucl. Mater. Energy* **12** 838
- [7] Kurzan B 2011 *Rev. Sci. Instrum.* **82** 103501
- [8] Sun H J *et al* 2017 *Plasma Phys. Control. Fusion* **59** 105010
- [9] Eich T *et al* 2011 *Phys. Rev. Lett.* **107** 215001
- [10] Pitcher C S *et al* 1997 *Plasma Phys. Control. Fusion* **39** 1129
- [11] McCormick K *et al* 1990 *J. Nucl. Mater.* **176&177** 89–101
- [12] Schneider P 2012 Characterization and scaling of the tokamak edge transport barrier *PhD Thesis* Ludwig–Maximilians–Universität, München
- [13] Stangeby P C 2000 *The Plasma Boundary of Magnetic Fusion Devices* (London: Institute of Physics Publishing)
- [14] Whyte D G *et al* 2010 *Nucl. Fusion* **50** 105005
- [15] Ryter F *et al* 2017 *Nucl. Fusion* **57** 016004
- [16] Manz P *et al* 2015 *Nucl. Fusion* **55** 083004
- [17] Happel T *et al* 2017 *Plasma Phys. Control. Fusion* **59** 014004
- [18] Kallenbach A *et al* 2018 *Plasma Phys. Control. Fusion* **60** 045006
- [19] LaBombard B 2001 *Phys. Plasma* **8** 2107
- [20] Carralero D 2015 *Phys. Rev. Lett.* **115** 215002
- [21] Schneider P A 2012 *Plasma Phys. Control. Fusion* **54** 105009